sortium for sharing analysis results; C. Allen and H. McClure of the Yerkes Primate Center, Atlanta, and W. Collignon and R. Bontrop of the Biomedical Primate Research Centre, Rijswijk, for tissue samples; T. Arendt of the Paul Flechsig Institute, Leipzig, for dissections; H. B. Fraser, H. Kaessmann, L. Vigilant, and all members of our laboratory for discussion; and the Max Planck Society and the Bundesministerium für Bildung und Forschung for financial support.

Supporting Online Material
www.sciencemag.org/cgi/content/full/1108296/DC1
Materials and Methods
Figs. S1 to S6
Tables S1 to S8
References and Notes

6 December 2004; accepted 6 April 2005
Published online 1 September 2005;
10.1126/science.1108296
Include this information when citing this paper.

Achieving Stability of Lipopolysaccharide-Induced NF-κB Activation

Markus W. Covert,* Thomas H. Leung,* Jahlionais E. Gaston, David Baltimore†

The activation dynamics of the transcription factor NF-κB exhibit damped oscillatory behavior when cells are stimulated by tumor necrosis factor–α (TNFα) but stable behavior when stimulated by lipopolysaccharide (LPS). LPS binding to Toll-like receptor 4 (TLR4) causes activation of NF-κB that requires two downstream pathways, each of which when isolated exhibits damped oscillatory behavior. Computational modeling of the two TLR4-dependent signaling pathways suggests that one pathway requires a time delay to establish early antiphase activation of NF-κB by the two pathways. The MyD88-independent pathway required Inferon regulatory factor 3–dependent expression of TNFα to activate NF-κB, and the time required for TNFα synthesis established the delay.

The transcription factor NF-κB regulates numerous genes that function in diverse processes, including inflammatory responses, immune system development, apoptosis, learning in the brain, and bone development (*1*). Aberrant NF-κB activity has been linked to oncogenesis, tumor progression, and resistance to chemotherapy (*2*). NF-κB has also been identified as a tumor promoter in inflammation-associated cancer (*3*). Understanding the specificity and temporal mechanisms that govern NF-κB activation may therefore be important in understanding cancer progression, and systems-based and computational approaches are being developed to address this issue (*4*, *5*).

The activity of NF-κB shows damped oscillatory behavior in cells stimulated with TNFα. Using a computational model coordinated to molecular and biochemical techniques, we have demonstrated that the oscillations in NF-κB activity are largely due to negative feedback by the NF-κB inhibitor protein IκBα (*6*). Another study performed in single cells has provided further evidence for these conclusions (*7*).

NF-κB mediates cellular responses to a wide variety of stimuli other than TNFα (*8*), and we wanted to determine whether NF-κB activation dynamics exhibited oscillations under other stimulation conditions. We observed non-oscillatory dynamics of active NF-κB when cells were stimulated with LPS (Fig. 1A). This difference in NF-κB activation could be linked to differences in the TNFα and LPS signaling pathways. Upon TNFα binding to the TNF receptor, the receptors aggregate and bind adaptor proteins, leading to activation of the IκB kinase (IKK) complex. Phosphorylation of IκB by IKK leads to ubiquitination and degradation of IκB and allows free NF-κB to bind target genes. One such target is IκBα, and its production results in a negative feedback loop (*9*–*11*).

In contrast, LPS signals through TLR4. TLR4 activates two downstream pathways, each of which is thought to directly activate NF-κB (*12*–*14*). The MyD88-dependent pathway recruits the kinases interleukin-1 receptor–associated kinase 1 (IRAK1) and IRAK4, which phosphorylate TNF receptor–associated factor 6 (TRAF6), leading to the activation of the IKK complex. The MyD88-independent pathway leading to NF-κB activation is not fully understood. The pathway is dependent on the TIR domain–containing adaptor inducing interferon-β (Trif) adaptor molecule, and Trif-related adaptor molecule (Tram), receptor-interactor protein 1 (RIP1), and RIP3 have been identified as important factors in the pathway (*15*–*17*). However, the end result of these pathways is the same as the end result of the TNFα-activated pathway: degradation of IκB, which is followed by activation of IκBα gene transcription. We monitored IκBα mRNA transcript and protein levels over a 180-min time course in LPS-stimulated wild-type cells and found that IκBα protein expression decreased and

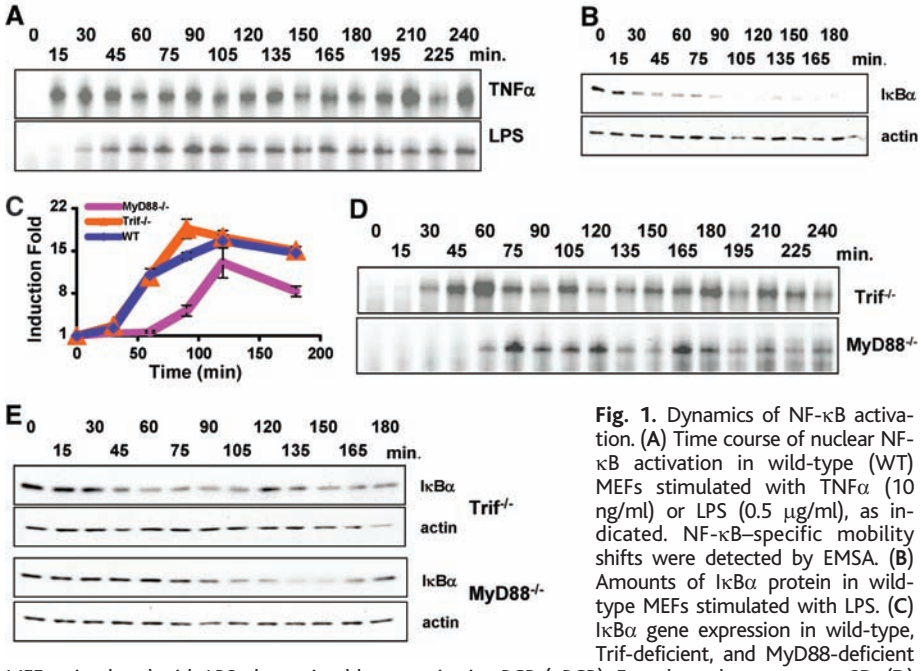

Fig. 1. Dynamics of NF-κB activation. (**A**) Time course of nuclear NF-κB activation in wild-type (WT) MEFs stimulated with TNFα (10 ng/ml) or LPS (0.5 μg/ml), as indicated. NF-κB–specific mobility shifts were detected by EMSA. (**B**) Amounts of IκBα protein in wild-type MEFs stimulated with LPS. (**C**) IκBα gene expression in wild-type, Trif-deficient, and MyD88-deficient MEFs stimulated with LPS, determined by quantitative PCR (qPCR). Error bars show means ± SD. (**D**) Time course of nuclear NF-κB activation in Trif-deficient and MyD88-deficient MEFs stimulated with LPS. (**E**) IκBα protein in Trif-deficient and MyD88-deficient MEFs stimulated with LPS. All experiments described here were repeated two or three times with a high degree of reproducibility.

Division of Biology, California Institute of Technology, Pasadena, CA 91125, USA.

*These authors contributed equally to this work.
†To whom correspondence should be addressed. E-mail: baltimo@caltech.edu

remained low, whereas mRNA expression increased and remained high (Fig. 1, B and C). Therefore, it remains puzzling that there are oscillations in NF-κB activity and IκBα protein expression after activation by TNF but not in cells stimulated with LPS.

NF-κB activation through the MyD88-dependent pathway occurs earlier than activation by the MyD88-independent pathway (*16*). This suggested that the non-oscillatory behavior of NF-κB activation through TLR4 could be due to the interaction of the two pathways. We monitored nuclear NF-κB activity over a 240-min time course in LPS-stimulated MyD88-deficient, Trif-deficient, and MyD88-Trif doubly deficient mouse embryo fibroblasts (MEFs) (Fig. 1D). LPS stimulation of MEFs that contained only one TLR4 pathway resulted in an oscillatory NF-κB activation response. LPS-stimulated cells deficient in both MyD88 and Trif showed no NF-κB activation. Moreover, in comparison with wild-type and Trif-deficient cells, LPS-stimulated MyD88-deficient cells were substantially slower to reach initial peak NF-κB activation. Over a 180-min time course, the amount of IκBα protein decreased in LPS-stimulated Trif- and MyD88-deficient cells, and the protein was then resynthesized, further confirming the underlying oscillatory NF-κB activation response. The period of oscillation for NF-κB activation (~45 min) was shorter than the period of the oscillation in IκBα abundance (~90 min) (Fig. 1E).

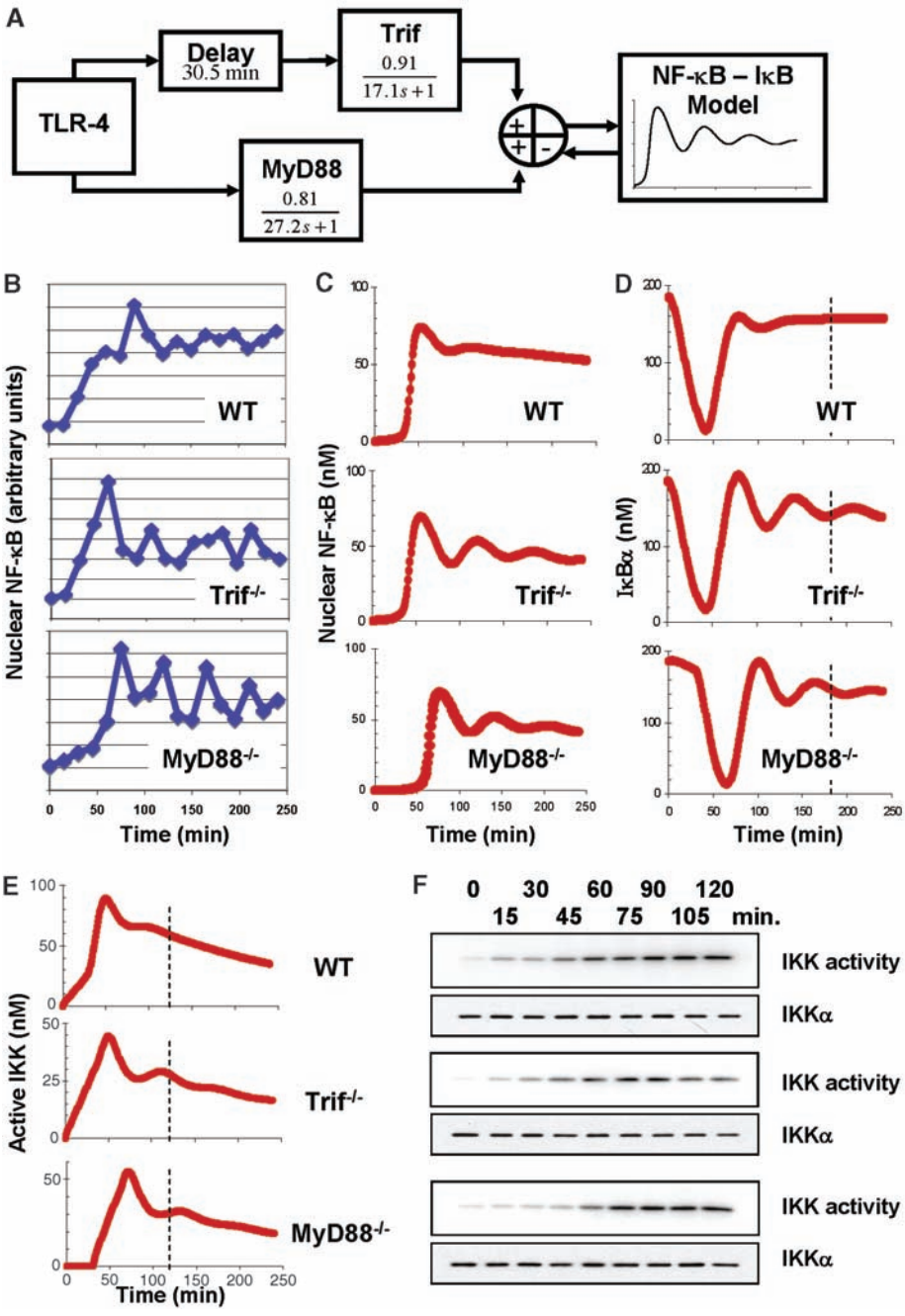

Fig. 2. Modeling the activation of NF-κB. (**A**) Schematic of a computational model of TLR4-dependent activation of NF-κB, partially represented as a block diagram (*27*). The blocks in the model contain first-order transfer functions of the form $K/(\tau s + 1)$, where K is called the steady state gain of the function and τ describes the time behavior. The parameter values were determined by (**B**) phosphoimager quantitation of NF-κB activation time courses (Fig. 1, A and D). "Trif" is used to denote the MyD88-independent pathway. (**C** to **E**) The predicted time courses of nuclear NF-κB activity (C), IκBα protein levels (D), and IKK activity (E). (**F**) IKK activity in wild-type, Trif-deficient, and MyD88-deficient cells. Dashed lines in (D) and (E) facilitate comparison of model predictions with data in Fig. 1E and (F).

A lag in NF-κB activation could occur in two ways: (i) The kinetics of the MyD88-independent pathway could simply be much slower than the kinetics of the MyD88-dependent pathway, or (ii) the MyD88-dependent and MyD88-independent pathways could display similar kinetics, in which case the initiation of the MyD88-independent pathway signaling must be delayed. We built a computational model to simulate NF-κB activation by TLR4 stimulation (Fig. 2A). The feedback loop between NF-κB and IκBα is a slightly modified version of our earlier model (*6*, *18*). Because the kinetic details of the MyD88-dependent and MyD88-independent pathways are not known, we described both pathways simply as first-order processes whose parameters were determined from our quantitated time course data (Fig. 2B). The model indicated that both the MyD88-independent and MyD88-dependent pathways are likely to have similar activation kinetics but that the MyD88-independent pathway requires a roughly 30-min time delay before it is activated (Fig. 2C).

This delay in pathway activation may occur at the level of IKK (Fig. 2E). We therefore monitored IKK activity in LPS-stimulated MyD88-deficient, Trif-deficient, and wild-type MEFs (Fig. 2F). IKK activation in wild-type and Trif-deficient MEFs began as early as 15 min after stimulation of cells with LPS and was sustained until 90 min. At that point, IKK activity in wild-type MEFs continued to increase, whereas IKK activity in Trif-deficient cells decreased. Furthermore, IKK activity in MyD88-deficient MEFs began to increase at 45 min. In contrast, TNFα-dependent activation of IKK reaches peak activity between 5 and 10 min and is inactive by 30 min (*19*, *20*). This difference in the length of IKK activity may help explain the difference in period length between nuclear NF-κB activity and IκBα protein levels for TLR4 stimulation. In Trif-deficient cells, IKK activity remains high through two complete oscillations of nuclear

NF-κB activity. This suggests that the oscillations in nuclear NF-κB activity are not due solely to IκBα protein abundance.

The computational model is necessarily minimal with respect to parameters and was derived primarily from the quantitative electromobility shift assay (EMSA) data. As such, the model fails to predict the discrepancy in period for IκBα protein synthesis and NF-κB activation, as well as the extended activation of IKK. However, the IκBα protein synthesis data qualitatively agrees with our model's prediction that IκBα protein levels would oscillate in the knockout cells but not in the wild-type cells (Figs. 1E and 2D) and the IKK activation data supports the prediction that the MyD88-independent pathway requires a time delay for activation (Fig. 2, E and F).

This delay might occur if NF-κB activation by the MyD88-independent pathway required protein synthesis. Thus, we pretreated wild-type, MyD88-deficient, Trif-deficient, and MyD88-Trif doubly deficient cells with cycloheximide before LPS stimulation, and monitored NF-κB activation over a 135-min time course (Fig. 3A). In LPS-stimulated wild-type or Trif-deficient cells, cycloheximide pretreatment triggered activation of NF-κB greater than that in wild-type cells, and MyD88-Trif doubly deficient cells demonstrated no inducible NF-κB activation. However in LPS-stimulated MyD88-deficient cells, NF-κB activation was abolished. Thus, the MyD88-independent pathway appears to require protein synthesis to activate NF-κB.

We used microarray technology to compare gene expression levels in LPS-stimulated MyD88-deficient cells at 0 and 45 min. Increased transcription of seven genes—T cell costimulatory receptor 4-1BB, glycoprotein CD83, chemokine interferon-inducible protein 10 (IP-10), macrophage inflammatory protein (MIP)–1α, MIP-1β, and MIP-2, and TNFα—was detected and confirmed by quantitative polymerase chain reaction (qPCR) (P value < 0.001, fold change > 2) (table S2). The majority of the identified genes (4-1BB, IP-10, the MIPs, and TNFα) encode extracellular messengers. We therefore treated MyD88-deficient cells with neutralizing antibodies or soluble receptors specific to certain candidate genes, stimulated the cells with LPS, and monitored activation of NF-κB (Fig. 3B). In MyD88-deficient cells, only pretreatment with soluble TNF receptor blocked LPS-stimulated activation of NF-κB. We detected small concentrations of TNFα (<30 pg/ml) by enzyme-linked immunosorbent assay in the supernatant of LPS-stimulated MyD88-deficient cells. In addition, expression of TNFα transcript in LPS-stimulated MyD88-deficient cells was up-regulated between 13- and 58-fold before NF-κB was active (Fig. 3C). Thus, the Trif-dependent pathway activates TNFα production and secretion in an NF-κB–independent manner. The secreted TNFα binds its receptors on the cell leading to NF-κB activation.

Interferon-regulatory factor 3 (IRF3) is a MyD88-independent pathway-specific transcription factor that directly regulates early response genes (for example, those encoding interferon-β and IP-10) and is active within 30 min of LPS stimulation (*21*). Furthermore, the TNFα promoter has several potential IRF binding sites. We used a retrovirus expressing an RNA interference cassette to silence endogenous IRF3 protein expression (*22*) in MyD88-deficient MEFs. Protein immunoblotting showed that the virus decreased the amount of IRF3 to one-eighth that in control cells (Fig. 3D). Depletion of IRF3 impaired the activation of NF-κB. Thus, IRF3 appears to mediate the activation of TNFα in the MyD88-independent pathway.

Previous studies by two different groups suggested that Trif directly activates NF-κB by interacting with adaptor molecules TRAF6 and Tank-binding kinase 1 (TBK1) (*23*, *24*). However, LPS-stimulated TRAF6-deficient macrophages were still capable of NF-κB activation with similar kinetics to the MyD88-independent pathway, and TLR3 signaling, which is dependent on Trif, was also not affected (*25*). We suggest that the activation of NF-κB by the Trif-dependent pathway results by means of a secondary response through TNFα and IRF3, establishing an autocrine pathway for delayed NF-κB activation (Fig. 3E). The combination of two out-of-phase oscillatory-based responses appears to allow for the stable and consistent early NF-κB response to LPS.

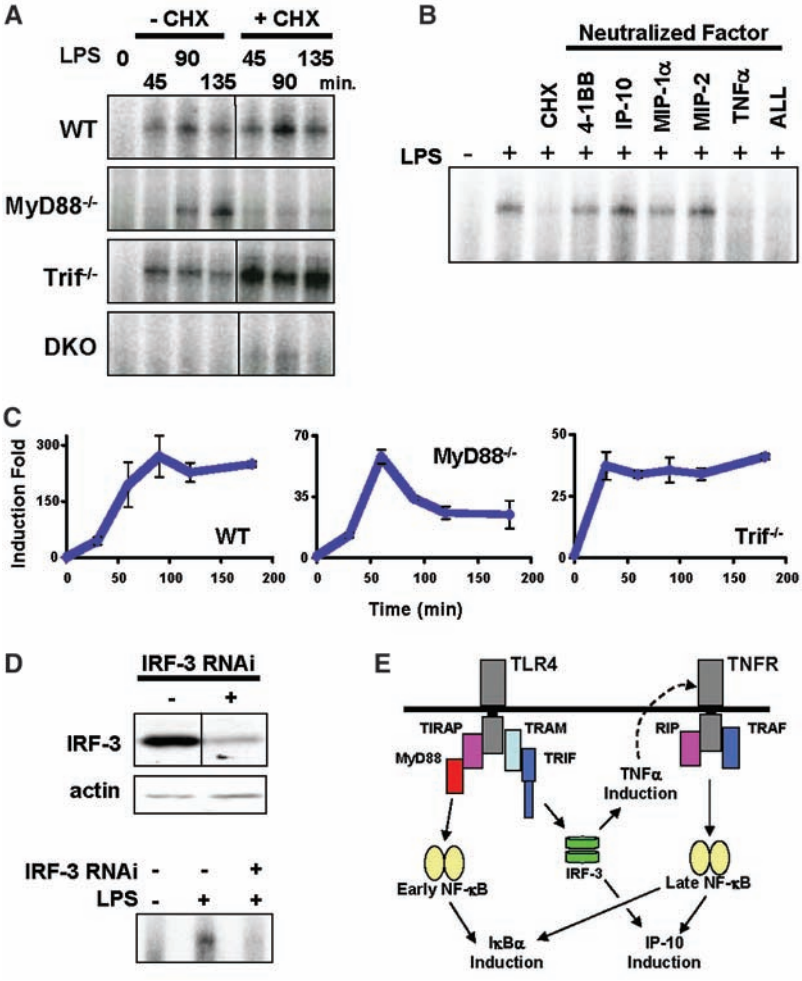

Fig. 3. MyD88-independent pathway activation of NF-κB requires IRF3-mediated expression of TNFα. Determination of LPS-induced nuclear NF-κB activity in MyD88-deficient MEFs by EMSA, where cells were (**A**) treated with cycloheximide (CHX) (25 μg/ml) for 60 min; (**B**) cotreated with one or all of the following: cycloheximide, soluble 4-1BB receptor (8 μg/ml), antibody to IP-10 (16.5 μg/ml), antibody to MIP-1α (2 μg/ml), antibody to MIP-2 (0.75 μg/ml), soluble TNFα receptor II (8.3 μg/ml); (**C**) infected with a lentiviral small interfering RNA construct to knock down IRF3 expression. (**D**) TNFα gene expression in wild-type, Trif-deficient, and MyD88-deficient MEFs stimulated with LPS, determined by qPCR. (**E**) Schematic of the proposed pathway for activation of NF-κB by means of Trif. Trif activates IRF3 through TBK1 and IκB kinase *i*, after which TNFα is expressed and secreted, activating NF-κB through the TNF pathway. TIRAP, Toll-interleukin 1 receptor domain–containing adaptor protein.

Nature often builds on a single mechanism to increase specificity and complexity. For transcription, increasingly complex genomes often contain a greater number of transcription factor family members than separate transcription factor families (*26*). This suggests that diversity within a gene family may provide specificity and versatility. Here the canonical pathway of NF-κB activation, which is activated once in cells treated with TNFα, is activated twice in response to TLR4 stimulation to create a distinct NF-κB activation profile.

References and Notes

1. S. Ghosh, M. J. May, E. B. Kopp, *Annu. Rev. Immunol.* **16**, 225 (1998).
2. A. S. Baldwin, *J. Clin. Invest.* **107**, 241 (2001).
3. E. Pikarsky *et al.*, *Nature* **431**, 461 (2004).
4. T. Bouwmeester *et al.*, *Nat. Cell Biol.* **6**, 97 (2004).
5. K. H. Cho, S. Y. Shin, H. W. Lee, O. Wolkenhauer, *Genome Res.* **13**, 2413 (2003).
6. A. Hoffmann, A. Levchenko, M. L. Scott, D. Baltimore, *Science* **298**, 1241 (2002).
7. D. E. Nelson *et al.*, *Science* **306**, 704 (2004).
8. M. S. Hayden, S. Ghosh, *Genes Dev.* **18**, 2195 (2004).
9. K. Brown, S. Park, T. Kanno, G. Franzoso, U. Siebenlist, *Proc. Natl. Acad. Sci. U.S.A.* **90**, 2532 (1993).
10. M. L. Scott, T. Fujita, H. C. Liou, G. P. Nolan, D. Baltimore, *Genes Dev.* **7**, 1266 (1993).
11. S. C. Sun, P. A. Ganchi, D. W. Ballard, W. C. Greene, *Science* **259**, 1912 (1993).
12. K. Kawasaki, H. Nogawa, M. Nishijima, *J. Immunol.* **170**, 413 (2003).
13. G. M. Barton, R. Medzhitov, *Science* **300**, 1524 (2003).
14. S. Akira, K. Takeda, T. Kaisho, *Nat. Immunol.* **2**, 675 (2001).
15. E. Meylan *et al.*, *Nat. Immunol.* **5**, 503 (2004).
16. M. Yamamoto *et al.*, *Science* **301**, 640 (2003).
17. M. Yamamoto *et al.*, *Nat. Immunol.* **4**, 1144 (2003).
18. Materials and methods are available as supporting material on *Science* Online.
19. J. A. DiDonato, M. Hayakawa, D. M. Rothwarf, E. Zandi, M. Karin, *Nature* **388**, 548 (1997).
20. F. Mercurio *et al.*, *Science* **278**, 860 (1997).
21. S. Doyle *et al.*, *Immunity* **17**, 251 (2002).
22. T. H. Leung, A. Hoffmann, D. Baltimore, *Cell* **118**, 453 (2004).
23. Z. Jiang, T. W. Mak, G. Sen, X. Li, *Proc. Natl. Acad. Sci. U.S.A.* **101**, 3533 (2004).
24. S. Sato *et al.*, *J. Immunol.* **171**, 4304 (2003).
25. J. Gohda, T. Matsumura, J. Inoue, *J. Immunol.* **173**, 2913 (2004).
26. E. S. Lander *et al.*, *Nature* **409**, 860 (2001).
27. D. E. Seborg, T. F. Edgar, D. A. Mellichamp, *Process Dynamics and Control, Wiley Series in Chemical Engineering* (John Wiley & Sons, New York, 1989), pp. 7–130.

28. We thank M. Yamamoto and S. Akira for generously providing the MEFs; M. Boldin, M. Meffert, and A. Hoffmann for valuable discussions; and the Millard and Muriel Jacobs Genetics and Genomics Laboratory at the California Institute of Technology for assistance with the gene expression study. This work was funded by the NIH (GM039458-21). M.W.C. is a Robert Black Fellow supported by the Damon Runyon Cancer Research Foundation (DRG-#1835-04). T.H.L. is a student in the UCLA–California Institute of Technology Medical Scientist Training Program and supported by the Achievement Rewards for College Scientists foundation.

Supporting Online Material

www.sciencemag.org/cgi/content/full/309/5742/1854/DC1
Materials and Methods
Fig. S1
Tables S1 and S2
References

15 March 2005; accepted 28 July 2005
10.1126/science.1112304

Stimulus Specificity of Gene Expression Programs Determined by Temporal Control of IKK Activity

Shannon L. Werner,* Derren Barken,* Alexander Hoffmann†

A small number of mammalian signaling pathways mediate a myriad of distinct physiological responses to diverse cellular stimuli. Temporal control of the signaling module that contains IκB kinase (IKK), its substrate inhibitor of NF-κB (IκB), and the key inflammatory transcription factor NF-κB can allow for selective gene activation. We have demonstrated that different inflammatory stimuli induce distinct IKK profiles, and we examined the underlying molecular mechanisms. Although tumor necrosis factor–α (TNFα)–induced IKK activity was rapidly attenuated by negative feedback, lipopolysaccharide (LPS) signaling and LPS-specific gene expression programs were dependent on a cytokine-mediated positive feedback mechanism. Thus, the distinct biological responses to LPS and TNFα depend on signaling pathway–specific mechanisms that regulate the temporal profile of IKK activity.

The evolutionarily conserved, signal-responsive transcription factor NF-κB plays a role in a myriad of physiological functions. These include lymphoid tissue development, immune, inflammatory, and environmental stress responses, and neuronal signaling (*1*, *2*). A number of human pathologies are caused by the impairment of signal-responsive NF-κB regulation, including chronic inflammatory diseases (*3*) and cancers (*4*). Thus, mechanisms that regulate NF-κB activity and allow it to control stimulus-specific physiological responses are of pressing clinical relevance (*5*, *6*) and are also of interest as a model system for studies of complex mammalian signaling systems.

NF-κB is held in an inactive state by association with one of three IκB proteins. In response to stimulation, the IκB kinase (IKK) phosphorylates NF-κB-bound IκB proteins, targeting them for proteolysis through the ubiquitin-proteasome pathway (*7*). A mathematical model based on ordinary differential equations recapitulated signaling of the IKK-IκB-NF-κB signaling module in response to the inflammatory cytokine tumor necrosis factor–α (TNFα) in murine embryonic fibroblasts (MEFs) (*8*). This model predicted dynamic signaling behavior resulting from IκB resynthesis, as observed biochemically (*8*) or in single-cell real-time imaging studies (*9*). Further refinements of the model have led to correct predictions of cross-regulation between IκB family members (*10*) and have uncovered important negative feedback mediated by the IκBε isoform (*11*).

The functional pleiotropism of NF-κB is based on the responsiveness of IKK to diverse signals transduced by plasma membrane–bound receptors or subcellular organelles (Fig. 1A) (*12*). Although different stimuli activate the same IKK-IκB-NF-κB signaling module, they elicit different gene expression programs. Because temporal control of NF-κB activity can lead to selective gene expression (*8*), we reasoned that stimulus-specific temporal control of IKK activity might allow for distinct biological responses if signal processing within the IKK-IκB-NF-κB signaling module resulted in distinct NF-κB activity profiles. To examine the signal processing characteristics of the signaling module, we generated a collection of potential IKK profiles with a simple algorithm (Fig. 1B). The algorithm allows for variable rises in IKK activity (over a time period of a = 0, 60, 120, or 240 min), a first plateau of various amplitudes (x = 4, 12, 34, or 101 nM) and durations (b = 0, 5, 15, 30, 60, or 120 min), variable decays (over a time period of c = 0, 60, 120, or 240 min), and a second, equal or lower, plateau of activity at or above baseline (y = 1, 4, 12, 34, or 101 nM).

The resulting comprehensive library of 687 distinct IKK activity profiles (fig. S1) served as inputs for computational simulations with our newly refined mathematical model (*13*). Each IKK input-NF-κB output pair (examples in Fig. 1C) reflects signal processing within the IKK-IκB-NF-κB signaling module. By grouping similar NF-κB activity profiles using standard K-means clustering, we investigated which IKK activity profiles are distinguished

Signaling Systems Laboratory, Department of Chemistry and Biochemistry, 9500 Gilman Drive, Mailcode 0375, La Jolla, CA 92093–0375, USA.

*These authors contributed equally to this work.
†To whom correspondence should be addressed. E-mail: ahoffmann@ucsd.edu